

## Pulse Shape Influence on the Accuracy of Z-scan Measurements\*

A. Dement'ev, A. Jovaiša

Institute of Physics, Savanorių av. 231, LT-02300 Vilnius  
aldement@ktl.mii.lt; anjova@ar.fi.lt

Received: 02.12.2004

Accepted: 16.03.2005

**Abstract.** Although the laser pulses with durations ranging from nanoseconds to femtoseconds and various pulse shapes are utilized for the Z-scan measurements, the influence of the temporal pulse shape on the measurement results is often neglected. In this paper, we tried to differentiate the influence of the temporal pulse shape on the common Z-scan technique with a small on-axis aperture in two cases: when the pulse peak intensity at the beam waist is known (for relatively long pulses), or when the total pulse energy and full width at half maximum (FWHM) of the correlation functions or FWHM of pulse durations are known (for short pulses).

**Keywords:** Z-scan, temporal pulse shape, nonlinearity coefficient.

### 1 Introduction

The Z-scan method [1–3] provides a simple technique for measurement of nonlinear properties of optical materials [4–7] and therefore it is becoming ever more popular and is also used for the measurements of nonlinear parameters of heterogeneous media [8–11]. A strong interest has lately been shown to the accuracy and reliability of the results obtained by means of this method, but the main attention was paid to the influence of the finite aperture size and similar problems [12, 13]. Although the lasers with pulse durations ranging from milliseconds to femtoseconds [14, 15] are routinely used for the Z-scan measurements, only the

---

\*The research was supported by Lithuanian State Science and Studies Foundation, project MODELITA, Reg. No. C-03048.

original papers [1–3], the review papers [4, 5] and a few others [16, 17] obviously indicate that the results must be averaged properly when the non-rectangular pulses are used. The latest works dealing with the Z-scan measurements do not pay much attention to the temporal pulse shapes [14, 15], also in cases when the Z-scan method with the temporal resolution [18] is employed. In well known handbooks [6, 7] there are only short indications that the normalized peak and valley transmittance is linearly dependent on the induced temporally averaged phase distortion. Without specifying explicitly how to average this phase, it may cause difficulties in obtaining correct results. Therefore, the detailed analysis of the Z-scan theoretical background with emphasis on the temporal pulse shape dependence can provide a useful insight into important aspects of this experimental tool that are usually overlooked.

In this paper, the results of the numerical analysis of the Z-scan experiments for thin samples with various temporal pulse shapes are presented for the case of long pulses, when the pulse peak intensity at the beam waist is known, and for the case of short pulses, when only the total pulse energy and the FWHM duration of the pulse or correlation functions are known.

## 2 Theoretical background of the Z-scan technique

The standard scheme for the Z-scan measurements is shown in Fig. 1. The Gaus-

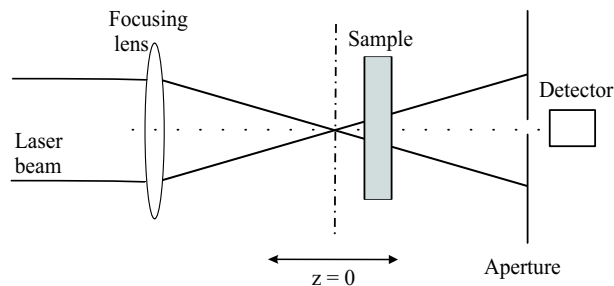


Fig. 1. Scheme of the experimental setup for the Z-scan measurement.

sian pump beam is focused by a lens to obtain a sufficiently small beam waist and high intensity. The sample is placed in the beam waist region and it is scanned along the  $z$ -axis. At a sufficiently large distance from the sample, an

aperture with an on-axis narrow opening and a detector that detects the energy changes behind the aperture are placed. When the sample is located far from the beam waist, where the beam intensity is low, the transmission through the aperture is normalized to unity. As the sample is shifted closer to the waist, the induced nonlinear absorption and nonlinear refraction index exert stronger influence upon the beam and the normalized transmittance curve takes characteristic shape [1–7]. For vivid explanation of the transmission changes due to this scan, a presentation of the sample of nonlinear medium as a thin nonlinear lens is commonly used. However, this explanation is not good in principle, because we cannot tell anything in general about the aberrated beam radius and how it changes during beam propagation without exact calculations [19]. The Z-scan technique allows determining the magnitude and sign of the nonlinear index change and the magnitude of the nonlinear absorption of the sample. For the simplicity we restrict ourselves only to the case of samples with Kerr nonlinearity, without nonlinear absorption. Z-scan is performed with laser beams, which have a highly directional nature. This direction of propagation is usually taken to be along the  $z$ -axis. Assuming a laser pulse propagating in the  $+z$  direction of the form

$$\tilde{\mathbf{E}}(x, y, z, t) = \text{Re}\{\hat{\mathbf{e}}E(x, y, z, t) \exp[i(k_0z - \omega t)]\}, \quad (1)$$

and employing the slowly varying envelope approximation (SVEA) the nonlinear Schrödinger equation (NSE) for slowly varying complex amplitude  $E(x, y, z, t)$  can be obtained [4, 6, 20]:

$$(\partial_x - v_g^{-1}\partial_t)E + \frac{ik_0''}{2}\partial_{tt}E + \frac{\Delta_{\perp}E}{2ik_0} + \frac{\alpha}{2}E = \frac{i\omega}{c}n_2|E|^2E, \quad (2)$$

where  $\hat{\mathbf{e}}$  is the unit polarization vector,  $k_0 = n_0(\omega)\omega/c$  is the modulus of the wave vector,  $\omega$  is the circular frequency of the rapidly oscillating laser wave,  $n_0(\omega)$  is the linear refractive index,  $v_g = (dk_0/d\omega)^{-1}$  is the group velocity,  $k_0'' = \partial_{\omega\omega}k$  is the group velocity dispersion (GVD) coefficient,  $\Delta_{\perp} = \partial_{xx} + \partial_{yy}$  is the transverse Laplacian,  $\alpha$  is the linear absorption coefficient,  $c$  is the velocity of light in vacuum,  $n_2$  is the nonlinear refraction index and the subscripts denote corresponding partial derivatives.

In vacuum  $v_g = c$ ,  $k_0'' = 0$ ,  $\alpha = 0$ ,  $n_0 = 1$ ,  $n_2 = 0$  and the simplest solution

of Eq. (2) is the circular Gaussian beam [4–6]:

$$E(r, z, t) = E_0(t) \frac{w_0}{w(z)} \exp \left[ -\frac{r^2}{w^2(z)} + \frac{ikr^2}{2R(z)} + i\psi(z) \right], \quad (3)$$

where  $r = \sqrt{x^2 + y^2}$  is the radial coordinate,  $E_0(t)$  is the field amplitude at the beam waist  $z = 0$  and contains the temporal envelope of the pulse,  $w_0$  is the radius at the beam waist,  $w^2(z) = w_0^2(1 + z^2/z_R^2)$  is the beam radius,  $k = 2\pi/\lambda$  is the wave number for the wavelength  $\lambda$  in the free space,  $R(z) = z(1 + z_R^2/z^2)$  is the wavefront curvature radius,  $z_R = kw_0^2/2$  is the Rayleigh length, and the term  $\psi(z) = -\arctan(z/z_R)$  contains the radially uniform phase variations along the  $z$ -axis.

We will assume that this Gaussian beam serves as a pump beam. Therefore Eq. (2) should be solved with that beam as a boundary condition entering the sample. The sample can be assumed as a thin sample if its thickness  $L$  is significantly less than the Rayleigh length  $z_R$  and the dispersion length  $L_D = |k''|\tau_L^2/2$  of the pump pulse of duration  $\tau_L$  with the Gaussian transverse intensity distribution. In this approximation second derivatives in Eq. (2) can be neglected and it is easy to determine that for the thin sample, the field amplitude  $E_e$  at the exit plane  $z + L \simeq z$  from the sample [1–3]

$$E_e(r, z, t) = E(r, z, t) e^{-\alpha L/2} e^{i\Delta\psi(r, z, t)} \quad (4)$$

contains the nonlinear phase shift

$$\Delta\psi(r, z, t) = \Delta\psi_0(z, t) \exp \left[ -\frac{2r^2}{w^2(z)} \right] \quad \text{with} \quad \Delta\psi_0(z, t) = \frac{\Delta\Psi_0(t)}{1 + z^2/z_R^2}, \quad (5)$$

where  $\Delta\Psi_0(t) = k\Delta n_0(t)L_{\text{eff}}$  is the on-axis phase shift at the beam waist,  $L_{\text{eff}} = (1 - e^{-\alpha L})/\alpha$ ,  $L$  is the sample length,  $\alpha$  is the linear absorption coefficient,  $\Delta n_0(t) = n_2|E(0, 0, t)|^2/2 = \gamma I_0(t)$  is the nonlinear change of refraction index,  $I_0(t) = (cn_0/8\pi)|E(0, 0, t)|^2$  is the on-axis intensity at the waist  $z = 0$  and  $\gamma = 4\pi n_2/cn_0$  is the Kerr nonlinear refraction index to be determined from the Z-scan transmission data.

The exact complex amplitude  $E_a(r, Z, t)$  at the aperture plane  $Z = z + d$  ( $d$  is the distance from the sample to the aperture) can be found using different methods for calculations of the aberrated beam propagation [21–24], and then

the normalized Z-scan transmittance through an aperture with radius  $a$  can be expressed as [1–3]

$$T(z) = \frac{\int_{-\infty}^{\infty} dt \int_0^a |E_a(r, Z, \Delta\Psi_0(t))|^2 r dr}{\int_{-\infty}^{\infty} dt \int_0^a |E_a(r, Z, \Delta\Psi_0(t) = 0)|^2 r dr}. \quad (6)$$

But the exact numerical calculation of the field  $E_a(r, Z, t)$  using the field amplitude (4) is rather complicated and requires much computational time for the calculation of  $E_a(r, Z, t)$  values for many space-time points  $z, t$  used in the Z-scan method.

Therefore for the Gaussian beam two approximate methods are widely used. In the case of nonlinear nonaberrational lens approach Fig. 2(a), the Gaussian beam behind the sample, which is treated as a thin ideal temporal lens, has the same beam radius and a different radius of curvature. Due to this, the position of the beam waist and intensity distribution in the far field are changing during the pulse.

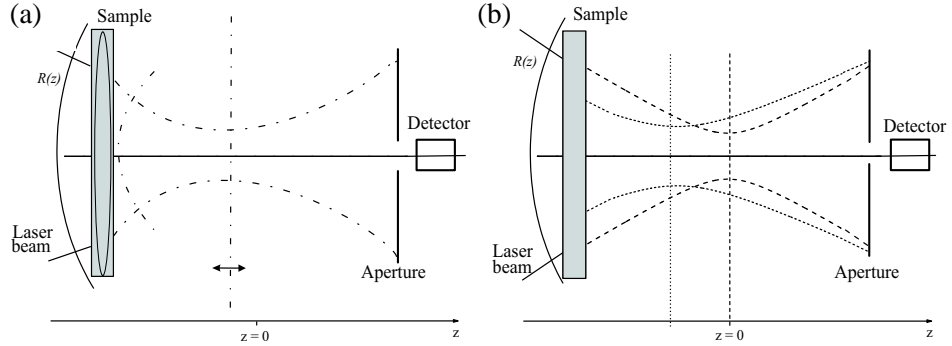


Fig. 2. Scheme of the setup for the Z-scan measurement and two different approaches for transmittance calculations: (a) thin nonlinear lens and (b) Gaussian decomposition.

The intensity distribution of the Gaussian beam is of the form

$$I(r, Z, t) = \frac{2P(t)}{\pi w^2(Z, t)} \exp\left[-\frac{2r^2}{w^2(Z, t)}\right], \quad (7)$$

where  $P(t)$  is the momentary power of the beam, and  $w(Z, t)$  is the beam width in the position  $Z$  of the aperture. If the aperture radius  $a \ll w(Z, t)$ , then  $\exp[-2a^2/w(Z, t)] \simeq 1$ , and the registered pulse power behind the aperture is

$$P_D(t) \approx \frac{2P(t)\pi a^2}{\pi w^2(Z, t)}. \quad (8)$$

For the calculation of the beam radius  $w(Z, t)$  at the aperture plane the well known *ABCD* law [25] can be used. In this approach the Gaussian beam is characterized in any position  $Z$  by the complex beam parameter

$$\frac{1}{q(Z, t)} = \frac{1}{R(Z, t)} + i \frac{\lambda}{\pi w^2(Z, t)}. \quad (9)$$

For the given beam parameter  $q$  on the initial plane  $z$  just before the sample, the beam parameter on any other plane is calculated using the *ABCD* law:

$$\tilde{q} = \frac{Aq + B}{Cq + D}. \quad (10)$$

The *ABCD* matrix for the beam propagation from the initial plane to the aperture plane consists of the product of two matrices corresponding to propagation through the nonlinear lens and the empty space. Transmittance of a simple linear lens is given by [25]

$$T_L = \exp \left[ -\frac{ikr^2}{2f} \right], \quad (11)$$

while the transmittance of the nonlinear sample as follows from (4) is related to the phase change by

$$T_S(t) = \exp [i\Delta\psi(r, z, t)]. \quad (12)$$

Thus, using the parabolic approximation in (5), the focal length of the nonaberrated nonlinear lens is

$$f_{NL}(z, t) = \frac{k w^2(z)}{4\Delta\psi_0(z, t)}. \quad (13)$$

Therefore, the propagation matrix from the initial plane  $z$  just before the sample through the thin lens with the focal length  $f_{NL}$  and the empty space of length  $d = Z - z$  from the sample to the aperture plane is given by

$$\begin{bmatrix} A & B \\ C & D \end{bmatrix} = \begin{bmatrix} 1 & d \\ 0 & 1 \end{bmatrix} \cdot \begin{bmatrix} 1 & 0 \\ -1/f_{NL} & 1 \end{bmatrix} = \begin{bmatrix} 1 - d/f_{NL} & d \\ -1/f_{NL} & 1 \end{bmatrix}. \quad (14)$$

The beam radius square on the plane  $Z$  of the aperture can be defined using formula [25]:

$$w_{NL}^2(Z) = w^2(z) \left[ \left( A + \frac{B}{R(z)} \right) + \left( \frac{\lambda B}{\pi w^2(z)} \right) \right]. \quad (15)$$

Taking into account (8) the transmittance (6) for a small aperture can be written in the form:

$$T_{NL}(z) = \frac{2a^2 \int_{-\infty}^{\infty} \frac{P(t)dt}{w_{NL}^2(Z,t)}}{2a^2 \int_{-\infty}^{\infty} \frac{P(t)dt}{w_L^2(Z)}} = \frac{\int_{-\infty}^{\infty} T_{NL}(z,t)P(t)dt}{\int_{-\infty}^{\infty} P(t)dt}, \quad (16)$$

where

$$T_{NL}(z,t) = \frac{w_L^2(Z)}{w_{NL}^2(Z,t)} = \frac{w_{NL}^2(Z, f_{NL} = \infty)}{w_{NL}^2(Z, f_{NL}(t))}. \quad (17)$$

Using these formulas, the transmittance for different distances  $d$  to the aperture can be easily calculated. For the case  $d \gg z_R$  ( $d$  is the distance from sample to the aperture plane) and small phase changes  $\Delta\Psi_0(t)$  it is easy to get, keeping only linear terms in  $\Delta\Psi_0(t)$ , simple enough formula for momentary transmittance:

$$T_{NL}(z,t) \simeq 1 + \frac{4(z/z_R)\Delta\Psi_0(t)}{(1 + z^2/z_R^2)^2}. \quad (18)$$

Now it is very clear what type of temporal averaging should be introduced for getting true normalized energy transmittance through the small aperture:

$$T_{NL}(z) \simeq 1 + \frac{4(z/z_R)\langle\Delta\Psi_0(t)\rangle}{(1 + z^2/z_R^2)^2}, \quad (19)$$

where

$$\langle\Delta\Psi_0(t)\rangle = \frac{\int_{-\infty}^{\infty} \Delta\Psi_0(t)P(t)dt}{\int_{-\infty}^{\infty} P(t)dt} \quad (20)$$

is the power-weighted time-averaged on-axial nonlinear phase change at the beam waist.

It should be noted that analogous ideal thin lens consideration was used previously for a thermal lens [26], but it was understood clearly enough that such approach is insufficiently precise and that a more elaborate approach, which takes into account aberrations of thermal lens, should be used. In spite of this knowledge, slightly different expression for a nonlinear lens transmittance is sometimes used for Z-scan measurement data processing [27, 28].

Transmittance curves calculated using formula (19) are presented in Fig. 3(a). It is seen that the peak in the transmission curve emerges first as the sample with negative  $n_2$  approaches the beam waist from the left, and then the valley appears after the sample passes through the waist.

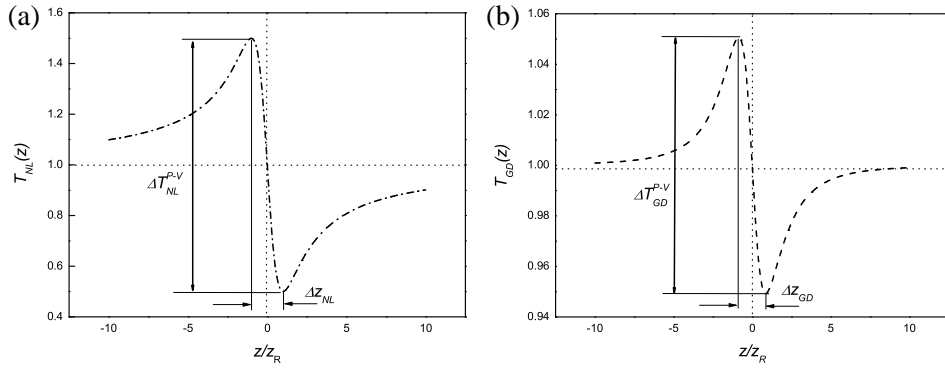


Fig. 3. The Z-scan transmittance through a small aperture for a thin nonlinear medium with negative  $\langle \Delta\Psi_0(t) \rangle = -0.25$  as calculated using the methods of the nonaberrated nonlinear lens approximation (a) and Gaussian beam decomposition (b).

The sample nonlinearity is calculated from the difference between the highest (peak) and the lowest (valley) transmission values denoted as  $\Delta T_{p-v}$ . The view would be opposite for the positive nonlinear refraction index because the sample would act as a focusing lens in this case. Qualitatively, this dependence can be explained as follows. The sample acts as the negative lens, and for negative  $z$  the enlarged beam waist is shifted towards the positive  $z$  coordinate. Therefore, the beam width beside the aperture becomes smaller and transmittance increases. At the waist, the sample has almost no effect because the curvature radius is infinite in this position. After the sample passes through the waist and moves toward the

aperture, it increases the beam divergence and thus decreases the transmission through the aperture.

As we will see somewhat later, qualitatively analogous transmittance curves are obtained using the standard for Z-scan Gaussian beam decomposition (GD) method [1–3]. Therefore, practically in all papers the explanation of transmittance curves is given usually in terms of an ideal (nonabberational) nonlinear lens, which is not true in general.

The Gaussian beam decomposition (GD) method takes into account special type of the aberrations induced in Kerr media by Gaussian beam. The GD method works as follows: the nonlinear phase term in (4) is decomposed into the Taylor series

$$\exp(i\Delta\psi(z, r, t)) = \sum_{m=0}^{\infty} \frac{[i\Delta\psi_0(z, t)]^m}{m!} \exp\left[-\frac{2mr^2}{w^2(z)}\right]. \quad (21)$$

This means that behind the thin nonlinear sample the incoming Gaussian beam is decomposed into the sum of Gaussian beams with the same curvature radius  $R(z)$  and different radius  $w_m(z) = w(z)/\sqrt{2m+1}$ :

$$E_e(r, z, t) = e^{-\alpha L/2} \sum_{m=0}^{\infty} E_0(t) \frac{w_0}{w(z)} \frac{[i\Delta\psi_0(z, t)]^m}{m!} \exp\left[\frac{-2r^2}{w_m^2(z)} + \frac{ikr}{2R(z)} + i\psi(z)\right]. \quad (22)$$

Using the *ABCD* law for each Gaussian beam propagation to the aperture plane with matrix

$$\begin{bmatrix} A & B \\ C & D \end{bmatrix} = \begin{bmatrix} 1 & d \\ 0 & 1 \end{bmatrix} \quad (23)$$

the field pattern of the aberrated beam at the aperture can be expressed as [1–3]:

$$E_a(r, z, t) = E(r=0, z, t) e^{-\alpha L/2} \sum_{m=0}^{\infty} \frac{[i\Delta\psi_0(z, t)]^m}{m!} \frac{w_{m0}}{w_m} \exp\left(-\frac{r^2}{w_m^2} + \frac{ikr^2}{2R_m} + i\theta_m\right), \quad (24)$$

where

$$w_{m0}^2 = \frac{w^2(z)}{2m+1}, \quad w_m^2 = w_{m0}^2 \left[ g^2 + \frac{d^2}{d_m^2} \right], \quad R_m = d \left[ 1 - \frac{g}{g^2 + d^2/d_m^2} \right]^{-1}$$

$$d_m = \frac{kw_{m0}^2}{2}, \quad g = 1 + \frac{d}{R(z)}, \quad \theta_m = \tan^{-1} \left[ \frac{d}{gd_m} \right].$$

In case of a small nonlinear phase change ( $|\Delta\Psi_0(t)| \ll 1$ ), using the far-field condition  $d \gg z_R$  and keeping linear in  $\Delta\Psi_0(t)$  terms only, the normalized Z-scan temporal transmittance can be written as [1–3]

$$T_{GD}(z, \Delta\Psi_0(t)) \simeq 1 + \frac{4(z/z_R)\Delta\Psi_0(t)}{(9 + z^2/z_R^2)(1 + z^2/z_R^2)}, \quad (25)$$

Normalized energy transmittance  $T_{GD}(z)$  will be defined now by the same formula, only  $\Delta\Psi_0(t)$  should be changed to  $\langle \Delta\Psi_0(t) \rangle$  determined by (20)

Thus, in the Gaussian decomposition method (Fig. 2(b)), the temporal dependence of the transmittance through the aperture is the result of interference of two Gaussian beams behind the sample – the slightly attenuated initial Gaussian pump beam and the additional Gaussian beam with the same (as for pump beam) curvature radius  $R(z)$  and smaller beam radius  $w_1(z)$ . It should be noted that only their amplitudes are changing in time, the positions and sizes of their waists are unchanged during the pulse.

Z-scan curves obtained by both methods look very alike for the positions and values of transmittance maxima and minima are different. What is more important, the transmittance peak and valley difference given by the Gaussian decomposition theory is a few times lower than that calculated for the nonlinear lens (Fig. 3) because the effects of the aberrations are intrinsically included in the Gaussian decomposition method. Therefore, below we will present results for different pulse shapes calculated using the Gaussian decomposition method only, omitting index GD in corresponding expressions.

### 3 Influence of the pulse shape

Many pulse shapes encountered in the Z-scan experiments can be described by super-Gaussian

$$f_j^{(SG)}(t) = \exp \left\{ -[\mu_S(t - t_{0j})/\tau_{0j}]^{2S} \right\}, \quad S = 1, 2, 3, \dots, \quad (26)$$

and asymmetrical pulses [29]

$$f_j^{(A)}(t) = \frac{\exp(at_m/\tau_{0j}) + \exp(-bt_m/\tau_{0j})}{\exp[a(t + t_m)/\tau_{0j}] + \exp[-b(t + t_m)/\tau_{0j}]}, \quad (27)$$

$$t_m = \frac{\ln(b/a)}{a+b} \tau_{0j}, \quad a > 0, b > 0.$$

In case of  $\mu_1 = 1.1774$  and  $\mu_2 = 1.5345$ , we have the Gaussian and lowest-order super-Gaussian pulses, and in case of  $a = b = 1.7628$  — the standard symmetric hyperbolic secant pulse with the duration  $\tau_{0j}$  as the full width at half maximum (FWHM) of the intensity profile. Several other temporal pulse shapes are plotted in Fig. 4. It should be noted that in Fig. 4, Fig. 5 and in Table 1  $\tau_0$  is the time normalization unit that is related to  $\tau_{0j}$  by some expressions, different for each pulse shape.

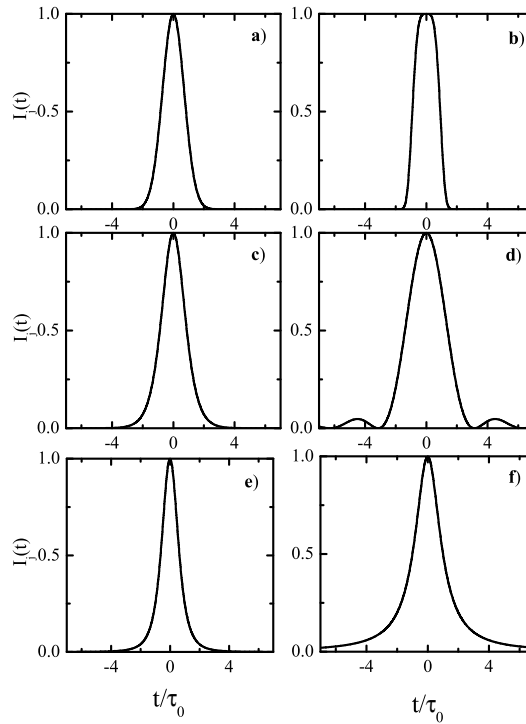


Fig. 4. Graphs of some typical temporal pulse shapes: (a) Gaussian, (b) super-Gaussian, (c) secant hyperbolic, (d) sinc, (e) Lorentzian-I, (f) Lorentzian-II.

It has been shown [1–3] that for a small phase change and a small aperture the magnitude of the sample nonlinearity can be determined in a straightforward manner by measuring the difference in the peak and valley transmittance values.

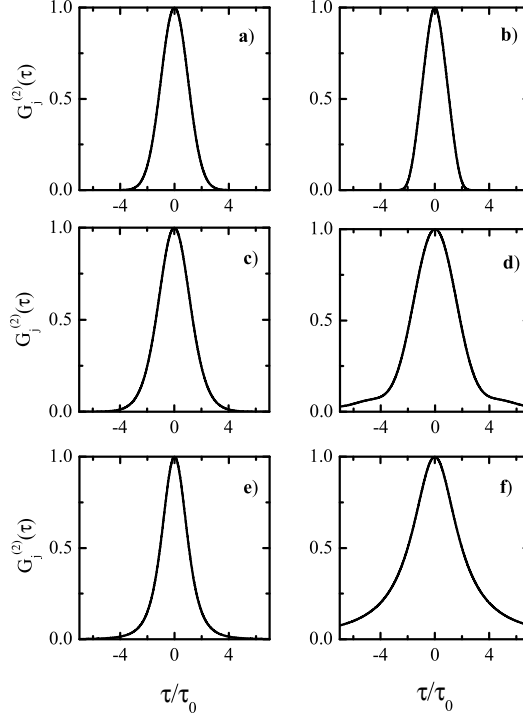


Fig. 5. Autocorrelation functions for various temporal pulse shapes: (a) Gaussian, (b) super-Gaussian, (c) secant hyperbolic, (d) sinc, (e) Lorentzian-I, (f) Lorentzian-II.

The peak and valley transmittance values can be calculated by solving equation  $dT(z)/dz = 0$  and for a given pulse shape

$$\Delta T_{p-v,j} = A_1 |\langle \Delta \Psi_{0j}(t) \rangle|, \quad (28)$$

where  $A_1 = 0.406$ ,  $\Delta \Psi_{0j}(t) = \Psi_{0j} F_j(t)$ ,  $\Psi_{0j} = \gamma k L_{\text{eff}} I_{0j}$  is the maximal nonlinear phase change,  $\gamma$  is the nonlinearity coefficient to be determined,  $k$  is the wave number,  $L_{\text{eff}}$  is the effective sample thickness,  $I_{0j}$  is the maximal intensity on the beam axis at the beam waist,  $F_j(t) = |f_j(t)|^2$  is the normalized (to unity at the peak) temporal shape of the pulse intensity. Taking into account (20), the difference in the peak and valley values for normalized energetical transmittance being measured by means of experiments can be written for a given temporal

Table 1. The correction coefficients  $\eta_j^{(1,2,3)}$  for the nonlinear index determined by Z-scan measurements with different temporal pulse shapes

Pulse shape	$f_j(t)$	$K_{Gj}$	$K_{Lj}$	$\eta_j^{(1)}$	$\eta_j^{(2)}$	$\eta_j^{(3)}$
Gaussian	$\exp[-(t/\tau_0)^2]$	1.67	1.18	1.41	0.27	0.38
Super-Gaussian	$\exp[-(t/\tau_0)^4]$	1.76	1.54	1.19	0.26	0.29
Sinc	$\frac{\sin(t/\tau_0)}{(t/\tau_0)}$	3.71	2.78	1.50	0.32	0.42
Secant hyperbolic	$\text{sech}(t/\tau_0)$	2.72	1.76	1.50	0.28	0.43
Lorentzian-I	$\frac{1}{1 + (t/\tau_0)^2}$	2.13	1.29	1.60	0.29	0.49
Lorentzian-II	$\frac{1}{\sqrt{1 + (t/\tau_0)^2}}$	4.00	2.00	2.00	0.39	0.79
Asymmetric sech	$a = 1.0, b = 1.0$	2.72	1.76	1.50	0.28	0.43
Asymmetric sech	$a = 1.0, b = 2.0$	1.94	1.19	1.51	0.28	0.46
Asymmetric sech	$a = 1.0, b = 5.0$	1.30	0.84	1.57	0.30	0.46

shape as:

$$\Delta T_{p-v,j} = \frac{A_1 |\gamma| k L_{\text{eff}} I_{0j}}{\eta_j^{(1)}}, \quad (29)$$

where values of the coefficient  $\eta_j^{(1)} = \frac{\int_{-\infty}^{\infty} |f_j(t')|^2 dt'}{\int_{-\infty}^{\infty} |f_j(t')|^4 dt'}$  depend on the temporal pulse shape and are given in Table 1.

Therefore, the value of the nonlinear refractive index determined by the Z-scan from the measured  $\Delta T_{p-v,j}$  is determined by the formula

$$|\gamma| = \eta_j^{(1)} \frac{\Delta T_{p-v,j}}{A_1 k L_{\text{eff}} I_{0j}} \quad (30)$$

It is easy to see from formulas (29) and (30) that for given maximal intensity  $I_{0j}$  the difference in the peak and valley transmittance values does not depend on the duration of pulses, it depends through the coefficient  $\eta_j^{(1)}$  on their shape only. The values of  $\eta_j^{(1)}$  for different pulses are presented in Table 1.

For short pulses only the total pulse energy

$$W_j = \frac{\pi w_{0j}^2}{2} I_{0j} \tau_0 \int_{-\infty}^{\infty} |f_j(t')|^2 dt' \quad (31)$$

and the FWHM duration  $\tau_{Gj} = K_{Gj} \tau_0$  of the autocorrelation function  $G_j^{(2)}(\tau) = \frac{\int_{-\infty}^{\infty} I_j(t) I_j(t + \tau) dt}{\int_{-\infty}^{\infty} I_j(t) I_j(t) dt}$  are often known (Fig. 5) [30]. Here  $K_{Gj}$  is the coefficient dependent on the pulse shape,  $\tau_0$  is the time normalization unit,  $t' = t/\tau_0$ . Graphs of the intensity and autocorrelation function for asymmetric secant pulses with different shapes are presented in Fig. 6.

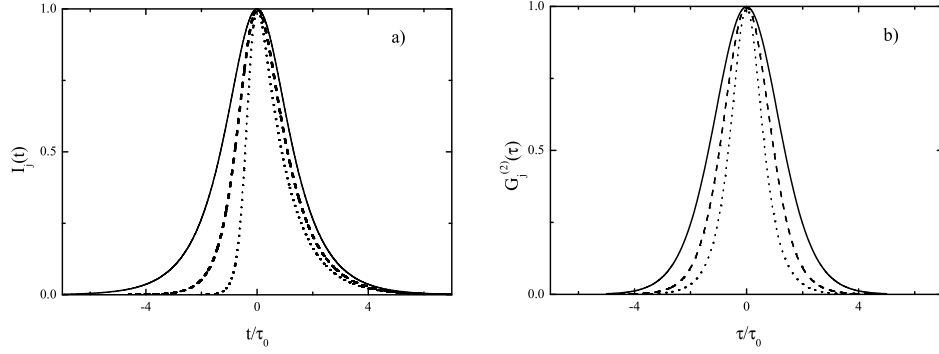


Fig. 6. Asymmetric secant pulse (a) and its autocorrelation functions (b) for  $a = 1$  and  $b = 1$  (solid),  $b = 2$  (dash) and  $b = 5$  (dot).

The following expression for the nonlinear refraction index can be written:

$$|\gamma| = \eta_j^{(2)} \frac{\lambda w_{0j}^2}{A_1 L_{\text{eff}}} \frac{\tau_{Gj}}{W_j} \Delta T_{p-v,j}, \quad (32)$$

where the coefficient dependent of the pulse shape is:

$$\eta_j^{(2)} = \left[ \int_{-\infty}^{\infty} |f_j(t')|^2 dt' \right]^2 \cdot \left[ 4K_{Gj} \int_{-\infty}^{\infty} |f_j(t')|^4 dt' \right]^{-1} \quad (33)$$

The numerically evaluated values of coefficients  $\eta_j^{(2)}$  for several pulse shapes are given in Table 1.

If the pulse duration  $\tau_{Lj} = K_{Lj}\tau_0$  is known, then the formula for nonlinear refraction index can be written as

$$|\gamma| = \eta_j^{(3)} \frac{\lambda w_{0j}^2}{A_1 L_{\text{eff}}} \frac{\tau_{Lj}}{W_j} \Delta T_{p-v,j}, \quad (34)$$

where the values for  $\eta_j^{(3)}$  can be obtained from  $\eta_j^{(2)}$  by changing  $K_{Gj}$  to  $K_{Lj}$ . The values of coefficients  $\eta_j^{(3)}$  are also given in Table 1. It can be seen from Table 1 that for the same measured experimental data (pulse energy and duration, peak-valley transmittance difference etc.) the value of sample nonlinear index may differ significantly if the pulse shape is not taken into account, if, e.g., the coefficients  $\eta_j^{(1,2,3)}$  are taken the same as for Gaussian pulse. Then the value of nonlinear index determined by such Z-scan measurements may differ from true one by the ratios  $\eta_j^{(1,2,3)}/\eta_G^{(1,2,3)}$  if pulse shape is not known exactly.

#### 4 Conclusions

We have numerically analyzed the influence of the temporal pulse shape in the Z-scan measurements for different cases: when the pulse peak intensity at the beam waist is known, and when the total pulse energy with the widths of its autocorrelation function or pulse durations are known. The results of the numerical investigation demonstrate that the temporal pulse shape has significant influence on the measurement results and therefore the values of the nonlinearity coefficient obtained by the Z-scan method can significantly differ from the real value if the proper pulse shape is not taken into account. The experimental tests of predicted results using the pulses of the SBS pulse compressor with different pulse shapes and duration [31, 32] are under the preparation.

#### References

1. M. Sheik-Bahae, A.A. Said, E.W. Van Stryland. High-sensitivity, single-beam  $n_2$  measurements, *Opt. Lett.*, **14**, pp.955–957, 1989.
2. M. Sheik-Bahae, A.A. Said, T.H. Wei, D.J. Hagan, E.W.V. Stryland. Sensitive measurement of  $n_2$  using a single beam, *Proc. SPIE*, **1438**, pp. 126–135, 1989.
3. M. Sheik-Bahae, A.A. Said, T.H. Wei, D.J. Hagan, E.W.V. Stryland. Sensitive measurement of optical nonlinearities using a single beam, *IEEE J. Quantum Electron.*, **26**, pp.760–769, 1990.

4. R.L. Sutherland. *Handbook of nonlinear optics*, Marcel Dekker, New York, 1996.
5. P.B. Chapple, J. Staromlynska, J.A. Hermann, T.J. McKay, R.G. McDuff. Single-beam Z-scan: measurement techniques and analysis, *J. Nonlin. Opt. Phys. Mat.*, **6**, pp. 251–293, 1997.
6. G.L. Wood, E.J. Sharp. Nonlinear optics, in: *Electro-Optics Handbook*, R.W. Waynant, M.N. Ediger (Eds.), McGraw-Hill, New York, pp. 13.1–13.28, 2000.
7. M. Sheik-Bahae, M.P. Hasselbeck. Third-order optical nonlinearities, in: *Handbook of Optics*, **IV**, M. Bass (Ed.), McGraw-Hill, New York, pp. 17.2–17.38, 2001.
8. K.S. Bindra, S.M. Oak, K.C. Rustagi. Intensity dependence of Z-scan in semiconductor-doped glasses for separation of third and fifth order contributions in the below band gap region, *Opt. Comm.*, **168**, pp. 219–225, 1999.
9. G. Battaglin, P. Calvelli, E. Cattaruzza, R. Polloni, E. Borsella, T. Cesca, F. Gonella, P. Mazzoldi. Laser-irradiation effects during Z-scan measurement on metal nanocluster composite glasses, *J. Opt. Soc. Am. B.*, **17**, pp. 213–218, 2000.
10. G.S. Maciel, C.B. de Araujo, A.A. Lipovskii, D.K. Tagantsev. Picosecond Z-scan measurements on a glass-ceramic containing sodium niobate nanocrystal, *Opt. Comm.*, **203**, pp. 441–444, 2002.
11. R.A. Ganeev, R.I. Tugushev, A.I. Ryasnyansky, T. Usmanov. Investigation of nonlinear refraction and nonlinear absorption of semiconductor nanoparticle solutions prepared by laser ablation, *J. Opt. A: Pure Appl. Opt.*, **5**, pp. 409–417, 2003.
12. X. Liu, S. Guo, H. Wang, N. Ming, L. Hou. Investigation of the influence of finite aperture size on the Z-scan transmittance curve. *J. Nonlin. Opt. Phys. Mat.*, **10**, pp. 431–439, 2001.
13. R. de Nalda, R. del Coso, J. Requejo-Isidro, J. Olivares, A. Suarez-Garcia, J. Solis, C. N. Afonso. Limits to the determination of the nonlinear refractive index by the Z-scan method. *J. Opt. Soc. Am. B*, **19**, pp. 289–296, 2002.
14. H.P. Li, C.H. Kam, Y.L. Lam, W. Ji. Femtosecond Z-scan measurements of nonlinear refraction in nonlinear optical crystals, *Opt. Mater.*, **15**, pp. 237–242, 2001.
15. L. De Boni, A.A. Andrade, L. Misoguti, C.R. Mendonça, S. Zilio. Z-scan measurements using femtosecond continuum generation, *Opt. Expr.*, **12**, pp. 3921–3927, 2004.
16. T. Shimada, N.A. Kurnit, M. Sheik-Bahae. Measurement of nonlinear index by a relay-imaged top-hat Z-scan technique, *Proc. SPIE*, **2714**, pp. 52–60, 1996.

17. W.P. Zang, J.G. Tian, Z.B. Liu, W.Y. Zhou, F. Song, C.P. Zhang. Analytic solutions to Z-scan characteristics of thick media with nonlinear refraction and nonlinear absorption, *J. Opt. Soc. Am. B*, **21**, pp. 63–66, 2004.
18. T. Kawazoe, H. Kawaguchi, J. Inoue, O. Haba, M. Ueda. Measurement of nonlinear refractive index by time-resolved Z-scan technique, *Opt. Commun.*, **160**, pp. 125–129, 1999.
19. A. Dement'ev, R. Navakas, R. Čiegis, G. Šilko. Numerical analysis of the ISO alternative methods for propagation factor measurements of coherent stigmatic beams, in: *Instruments and standard test procedures for laser beam and optics characterization, CHOCLAB II*, D. Nickel (Ed.), VDI-Technology center, Stuttgart, pp. 105–123, 2003.
20. M. Kolesik, J.V. Moloney. Nonlinear optical pulse propagation simulation: from Maxwell's to unidirectional equations, *Phys. Rev. E*, **70**, pp. 036604.1–036604.11, 2004.
21. S. Hughes, J.M. Burzler, G. Spruce, B.S. Wherrett. Fast Fourier transform techniques for efficient simulation of Z-scan measurements, *J. Opt. Soc. Am. B*, **12**, pp. 1888–1893, 1995.
22. A. Eriksson, M. Lindgren, S. Svensson, P.O. Arntzen. Numerical analysis of Z-scan experiments by use of a mode expansion, *J. Opt. Soc. Am. B*, **15**, pp. 810–816, 1998.
23. A. Dement'ev, R. Čiegis, G. Šilko. A tool for modeling optical beam propagation, *Informatica*, **13**, pp. 149–162, 2002.
24. B. Yao, L. Ren, X. Hou. Z-scan theory based on a diffraction model, *J. Opt. Soc. Am. B*, **20**, pp. 1290–1294, 2003.
25. Yu. A. Anan'ev. *Laser Resonators and the Beam Divergence Problem*, Adam Hilger, Bristol, 1992.
26. H.L. Fang, R.L. Swofford. Thermal lens in absorption spectroscopy, in: *Ultra-sensitive laser spectroscopy*, D.S. Kliger (Ed.), Academic Press, New York, 1983.
27. O.L. Antipov, A.V. Afanas'ev, G.A. Domrachev, W. Douglas, A.P. Zinov'ev, L.G. Klapshina, V.V. Semenov, Zh.Yu. Fominykh. Measurement of cubic nonlinear-optical susceptibility of new metallorganic polymer films and solutions, *Quant. Electr.*, **31**, pp. 432–436, 2001.
28. A.V. Afanas'ev, A.P. Zinoviev, O.L. Antipov, B.A. Bushuk, S.B. Bushuk, A.N. Rubinov, J.Yu. Fominih, L.G. Klapshina, G.A. Domrachev, W.E. Douglas. Picosecond Z-scan measurements of nonlinear optical susceptibility of films and solutions of novel organometallic polymers, *Opt. Comm.*, **201**, pp. 207–215, 2002.

29. J.-C. Diels, W. Rudolph. *Ultrashort Laser Pulse Phenomena. Fundamentals, Techniques and Applications on a Femtosecond Time Scale*, Academic Press, San Diego, 1996.
30. M.J. Shchelev. Picosecond electro-optical diagnostics in laser measurements, in: *Trudy FIAN*, N.G. Basov (Ed.), Nauka, Moscow, 1985.
31. A. Dement'ev, R. Buzelis, E. Kosenko, E. Murauskas, R. Navakas. Solid-state lasers with pulse compression by transient stimulated Brillouin and Raman scattering, in: *Proc. SPIE*, **4415**, pp. 92–97, 2001.
32. G.A. Pasmanik, E.I. Shklovsky, A.A. Shilov. Stimulated Brillouin Scattering Pulse Compression and Its Application in Lasers, in: *Phase Conjugate Laser Optics*, A. Brignon, J.P. Huignard (Eds.), John Willey & Sons, New Jersey, 2004.